PLOS ONE

RESEARCH ARTICLE

Nitrosative stress under microaerobic conditions triggers inositol metabolism in *Pseudomonas extremaustralis*

Esmeralda C. Solar Venero[1], Lucia Giambartolomei[2], Ezequiel Sosa[3], Darío Fernández do Porto[2,3], Nancy I. López[1,2☯], Paula M. Tribelli[1,2☯]*

1 IQUIBICEN-CONICET, Buenos Aires, Argentina, **2** Facultad de Ciencias Exactas y Naturales, Departamento de Química Biológica, Universidad de Buenos Aires, Buenos Aires, Argentina, **3** Instituto de Cálculo, Facultad de Ciencias Exactas y Naturales, UBA, Buenos Aires, Argentina

☯ These authors contributed equally to this work.
* paulatrib@qb.fcen.uba.ar

Citation: Venero ECS, Giambartolomei L, Sosa E, Fernández do Porto D, López NI, Tribelli PM (2024) Nitrosative stress under microaerobic conditions triggers inositol metabolism in *Pseudomonas extremaustralis*. PLoS ONE 19(5): e0301252. https://doi.org/10.1371/journal.pone.0301252

Editor: Abdelwahab Omri, Laurentian University, CANADA

Received: December 23, 2023

Accepted: March 13, 2024

Published: May 2, 2024

Data Availability Statement: RNAseq data were deposited in the European Molecular Biology Laboratory under accession number E-MTAB-11689 (https://www.ebi.ac.uk/biostudies/arrayexpress/studies/E-MTAB-11689).

Funding: This work was funded by grants from Universidad de Buenos Aires 20020170100310BA and 20020220400198BA and by the Consejo Nacional de Investigaciones Científicas y Técnicas (CONICET) Grant 11220200101436CO.

Abstract

Bacteria are exposed to reactive oxygen and nitrogen species that provoke oxidative and nitrosative stress which can lead to macromolecule damage. Coping with stress conditions involves the adjustment of cellular responses, which helps to address metabolic challenges. In this study, we performed a global transcriptomic analysis of the response of *Pseudomonas extremaustralis* to nitrosative stress, induced by S-nitrosoglutathione (GSNO), a nitric oxide donor, under microaerobic conditions. The analysis revealed the upregulation of genes associated with inositol catabolism; a compound widely distributed in nature whose metabolism in bacteria has aroused interest. The RNAseq data also showed heightened expression of genes involved in essential cellular processes like transcription, translation, amino acid transport and biosynthesis, as well as in stress resistance including iron-dependent superoxide dismutase, alkyl hydroperoxide reductase, thioredoxin, and glutathione S-transferase in response to GSNO. Furthermore, GSNO exposure differentially affected the expression of genes encoding nitrosylation target proteins, encompassing metalloproteins and proteins with free cysteine and /or tyrosine residues. Notably, genes associated with iron metabolism, such as pyoverdine synthesis and iron transporter genes, showed activation in the presence of GSNO, likely as response to enhanced protein turnover. Physiological assays demonstrated that *P. extremaustralis* can utilize inositol proficiently under both aerobic and microaerobic conditions, achieving growth comparable to glucose-supplemented cultures. Moreover, supplementing the culture medium with inositol enhances the stress tolerance of *P. extremaustralis* against combined oxidative-nitrosative stress. Concordant with the heightened expression of pyoverdine genes under nitrosative stress, elevated pyoverdine production was observed when *myo*-inositol was added to the culture medium. These findings highlight the influence of nitrosative stress on proteins susceptible to nitrosylation and iron metabolism. Furthermore, the activation of *myo*-inositol catabolism emerges as a protective mechanism against nitrosative stress, shedding light on this pathway in bacterial systems, and holding significance in the adaptation to unfavorable conditions.

Competing interests: The authors have declared that no competing interests exist.

Introduction

Bacterial survival and adaptability in changing environments depend on different resistance mechanisms against several stress agents. Free radicals are highly reactive species, mainly originated from energy producing processes like aerobic and anaerobic respiration, causing damage to different macromolecules. Reactive oxygen species (ROS) are produced during aerobic respiration, while anaerobic respiration, utilizing nitrate as electron acceptor, generates reactive nitrogen species (RNS). ROS and RNS trigger oxidative or nitrosative stress, respectively. RNS include nitric oxide (NO) and its derivatives peroxynitrite ($ONOO^-$), nitrosothiols formed through reaction with thiol groups, and nitrotyrosine from nitration of tyrosine by NO, $ONOO^-$ or NO_2^- [1–3]. Nitrosative and oxidative stress can also be induced from various environmental compounds, like pollutants, xenobiotics, and antimicrobials, and from UV radiation [4]. NO is also produced by the mammalian immune system and acts as a modulator molecule in both mammals and plants [5–7]. Nitrosative stress can lead to DNA and macromolecular damage, including protein oxidation. Some residues or structures are more susceptible to the RNS or ROS attack such as iron-sulfur (Fe-S) clusters, metal centers, tyrosine and cysteine residues, and thiols [8]. The radical attack to these residues or clusters results in both reversible and irreversible damage, leading to alterations in function and structure [9].

Pseudomonas species exhibit a wide variety of energy-generation metabolisms spanning from aerobic to anaerobic, involving NO_3^- reduction, complete denitrification process to N_2 and even fermentation of arginine or pyruvate [10,11]. These energy-generating pathways enable *Pseudomonas* species to thrive in diverse environmental niches, including soil, water, and host-associated habitats, and they play an integral role in the ecological and physiological success of these microorganisms. *Pseudomonas extremaustralis* is an Antarctic bacterium, capable to growth under different temperatures and oxygen availability. The denitrification process in this bacterium is incomplete, due to the absence of *nir* genes which encode the enzymes required for the reduction of NO_2^- to NO, but interestingly, harbors all the *nor* and *nos* genes associated with nitric and nitrous oxide reduction, respectively [12].

Bacterial adaptation to different stress conditions entails changes leading to solve metabolic and structural challenges, such as alterations or damage in DNA, RNA and proteins and envelopes, among others. Some strategies can involve the utilization of alternative pathways to exploit different carbon sources. Thus, when *P. putida* was grown at 10˚C, the uptake and assimilation of branched-chain amino acids alongside the activation of the 2-methylcitrate pathway to generate succinate and pyruvate has been identified as mechanism employed to cope with stress when central metabolism is downregulated [13]. Likewise, in cold conditions genes involved in primary metabolism were downregulated in *P. extremaustralis* whereas genes linked to ethanol oxidation were activated, showing that this secondary pathway resulted essential for cold growth [14]. In *P. aeruginosa*, it has been reported that under oxidative stress the glyoxylate shunt, an alternative to the tricarboxylic acid cycle, increases bacterial survival allowing the utilization of acetate and fatty acids as carbon sources [15].

Considering the importance of RNS derived from both anaerobic respiration and other biotic and abiotic environmental reactions, we evaluated the global transcriptomic response of *P. extremaustralis* to nitrosative stress under low O_2 tensions using S-nitrosoglutation (GSNO), as a NO donor compound. Our findings show that exposure to GSNO under microaerobic conditions prompted adjustments in central metabolic pathways including iron metabolism along with the upregulation of genes associated with the inositol catabolism. Notably, *myo*-inositol arises as a carbon source supporting *P. extremaustralis* growth and increased nitro-oxidative stress resistance and pyoverdine production. These findings highlight the versatility and adaptability of *P. extremaustralis* to withstand nitrosative stress, by displaying an

alternative metabolism, thus contributing to the understanding of the survival mechanisms employed by microorganisms in extreme environments.

Materials and methods

Strains and culture conditions

P. extremaustralis 14-3b (DSM 25547), a species isolated from the Antarctica [16] was used through the experiments. Bacterial cultures were grown in Lysogeny Broth medium (LB) at 30˚C. Microaerobic cultures were incubated in sealed bottles with a 1:2 medium-to-flask volume ratio and 50 rpm agitation. Microaerobic culture's medium was supplemented with 0.8 g/l KNO_3.

GSNO effect on *P. extremaustralis*' survival and growth was determined in microaerobic cultures exposed to 1, 10 and 100 μM of GSNO. Bacterial growth was evaluated by measurement of absorbance at optical density of 600 nm (OD600) after adding the different concentrations of GSNO at T = 0. Absorbance was monitored over 24 h at 30min intervals using an automated plate reader (BMG OPTIMA FLUOstar). For survival experiments, cultures were grown for 24h and further exposed to the different concentrations of GSNO for 1h. Afterwards, appropriate dilutions of control cultures (m-C) or cultures exposed to GSNO were plated in LB agar and incubated at 30˚C. Colony-forming units per ml (CFU / ml) was determined and the survival percentage was calculated with respect to control cultures.

RNA extraction and RNA library preparation

Liquid cultures were microaerobically grown in LB medium for 24 h and then incubated for 1 h with 100 μM S-nitrosoglutatione (GSNO, Sigma Aldrich) (m-NS condition) or with the addition of sterile water (m-C). Total RNA was isolated from 6 ml of *P. extremaustralis* m-C and m-NS cultures using the Trizol reagent (Invitrogen) [17]. Samples were treated with DNAse I and were validated using an Agilent 2100 Bioanalyzer (Agilent Technologies). To improve the quality of the readings, ribosomal RNA was depleted from the samples, using the RiboZERO Kit (Illumina), following the manufacturer's instructions. Libraries were prepared using the TruSeq RNA Library Prep Kit v2 (Illumina). Mass sequencing was performed using NextSeq 550 platform with a single-end protocol, in which the cDNA strand is sequenced from only one end. For each condition duplicated independent RNA extraction and libraries were used. rRNA depletion, library preparation and sequencing were performed by the Core Unit Systemmedizin (University of Würzburg, Germany).

RNAseq data analysis

Reads were preprocessed using the Trimmomatic tool [18] by eliminating adapters and low-quality sequences. Reads' quality was evaluated using the Fast QC tool (www.bioinformatics.babraham.ac.uk/projects/fastqc/). Quality information for sequencing data can be found in S1A Fig.

Reads alignment and assembly to the *P. extremaustralis* genome, transcript identification and abundance quantification was carried out using the Rockhopper software that use the Bowtie2, Bayesian and Anders and Huber approaches [19]. Reads were normalized per kilobase per million mapped reads (RPKM). Differential gene expression was considered only with $P < 0.05$ and $Q < 0.05$. Concordance between the independent replicates for each of the analyzed conditions was verified by performing a Spearman correlation analysis of normalized counts (S1B and S1C Fig).

Genes were assorted into functional classes using KEGG [20], MetaCyc [21] and String [22] tools.

Prediction of oxidation and nitrosylation targets

The Target-Pathogen tool [23] was used to identify proteins with possible oxidation and / or nitrosylation target sites (free Cys or Tyr residues or metal biding clusters) within the *P. extremaustralis* genome.

Comparative genome analysis

General genome sequence analysis was performed using the bioinformatics tools available on National Center for Biotechnology Information (www.ncbi.nlm.nih.gov), including BLAST (Basic Local Alignment Search Tool) [24]. We also used RAST (Rapid Annotation using Subsystem Technology) server [25] and *Pseudomonas* Genome Database (Pseudomonas.com, [26]). Genomes used, with corresponding GenBank accession numbers, were: *P. extremaustralis*: 14-3b (AHIP00000000.1), USBA 515 (FUYI01), DSM 17835^{T} (LT629689.1), 2E-UNGS (CP091043.1), CSW01(JAQKGS01),1906 (JARIXU01), NQ5 (JARBJR01) strains, *P. protegens* Pf-5 (CP000076.1), and *P. syringae* pv syringae B728a (CP000075.1).

Reverse transcription-quantitative polymerase chain reaction (RT qPCR)

Total RNA of *P. extremaustralis* microaerobic and m-NS cultures was isolated using the Total RNA Extraction Kit (RBC Biosciences). After treatment with DNaseI, cDNA was obtained using random hexamers (Promega) and Revert Aid reverse transcriptase (ThermoFisher Scientific) according to the manufacturer's instructions. RT-qPCR was performed using a MyiQ2 Real-Time PCR Detection System (Bio-Rad Laboratories, Hercules, USA) and Real-Time PCR mix (EvaGreen qPCR Mix Plus no ROX). The expression of selected genes was evaluated using the following primers: *motB* forward 5′ CAACGCCAGCAACAAAGACA 3′ and reverse 5′ CTTCG GAAAACCGCGCATC 3′; *hbo* forward 5′ CGAGCCTAAGAGCAACACCA 3′ and reverse 5′TGAAT AGGCTGTCGGCACTG 3′ and *flaB* forward 5' CGTAACCAGCGCTGACATGGCTC 3' and reverse 5' GACAGGATCGCAGTGGAAGCCGA 3'. Expression of the 16S rRNA gene was used for normalization of target genes expression levels in each condition, obtained using primers forward 5′ AGCTTGCTCCTTGATTCAGC 3′ and reverse 5′ AAGGGCCATGATGACTTGAC′ 3. The cycling conditions were as follows: denaturation at 95˚C for 15 min, 40 cycles at 95˚C for 25 s, 60˚C for 15 s, and 72˚C for 15 s, with fluorescence acquisition at 80˚C in single mode. The $2^{-\Delta\Delta CT}$ method [27] was used to calculate the relative fold gene expression of individual genes.

Bacterial growth using *myo*-inositol as sole carbon source

Myo-inositol metabolism was evaluated in E2 medium [28] supplemented with 10 g/l of *myo*-inositol or glucose under aerobic and microaerobic conditions. Microaerobic cultures were performed as described above while for aerobic experiments, cultures were incubated in Erlenmeyer flasks using 1:10 medium-to-flask volume ratio and 200 rpm agitation. Aerobic and microaerobic cultures were incubated for 24h and 48h, respectively, at 30^{o}C.

Biofilm formation was assayed in E2 medium supplemented with *myo*-inositol or glucose and KNO_3 in polystyrene microtiter plates with an initial OD_{600nm} of 0.025. After 48h of static incubation at 30˚C, OD_{600nm} of planktonic cells (planktonic cells absorbance, PCA) was measured and biofilms were quantified using the standard crystal violet method [29]. Briefly, attached cells were stained with 200 μl of 0.1% crystal violet, further washed and the colorant was solubilized with absolute ethanol. Crystal violet solution was transferred to flat bottom

microtiter plates and OD_{570nm} (Crystal violet absorbance CVA) was measured with a BMG OPTIMA FLUOstar microplate reader. Biofilm formation index was defined as CVA/PCA.

Pyoverdine production

Pyoverdine production of microaerobic cultures was analyzed in iron-limited E2 medium, without microelements, supplemented with *myo*-inositol or glucose as carbon source and KNO_3. After 48h pyoverdines in the culture supernatants were determined by measuring integrated fluorescence emission between 445–460 nm after excitation at 420 nm [30,31]. The values were expressed relative to cell dry weight per ml.

Survival and stress experiments

P. extremaustralis was cultured for 48h under microaerobic conditions in E2 cultures supplemented with *myo*-inositol or glucose and KNO_3 (0.8 g/l). Cultures were exposed to 100 μM GSNO (m-NS) for 1h and cell viability was determined in plate assay.

Growth inhibition in response to oxidative or combined nitro-oxidative stress was evaluated by filter disk assay by growing *P. extremaustralis* in E2 medium supplemented with glucose or *myo*-inositol and increasing KNO_3 concentrations of 0.8, 1.5 and 2.5 g/l that led to nitrite accumulation. Control cultures without nitrate were performed (oxidative stress only). LB plates were seeded with the different cultures and Whatman n˚ 1 filter discs (6 mm) were impregnated with 5 μl of 30% (v/v) H_2O_2 (Merck) as previously described [32]. Plates were incubated overnight at 30ºC, and the diameter of the halo was determined using the software ImageJ [33]. Nitrite concentration in the supernatant of cultures was determined following the method described by [34] and values were normalized to cell dry weight.

Flow cytometry analysis

The pool of reduced thiol molecules was analyzed through flow cytometry assays using Mercury Orange, a fluorescent thiol-reactive dye that showed preference for free reduced thiols [35]. Cultures grown 48h with glucose or inositol as carbon source were exposed to 100 μM of GSNO. Additionally, control cultures without GSNO were used. Afterwards, cells were washed and resuspended in 1 ml of physiological saline solution, OD_{600nm} was adjusted to 0,2 and cells were further incubated for 1 h (in darkness) 1 mM Mercury Orange dye (Sigma).

A FACS AriaI BD cell sorter (BD, Bioscience) with FIT-C (Blue Diode at 488 nm) and FL2 (585–542 nm) filters was used andat least 10,000 events in each tube were measured. The autofluorescence of the bacterial population was detected with non-stained cells and used to determine the positive fluorescence. The geometric mean (Gm) and the percentage of cells with positive fluorescence signal (% positive cells) were determined using Floreada.IO software (Joseph Trotter).

Statistical analysis

Differences between means were determined through the Student's t test with confidence levels at $> 95\%$ in which $P < 0.05$ was considered as statistically significant. A Fisher's exact test was performed to analyze the nitrosylation targets proteins. 1 or 2-ways ANOVA with multiple comparison were used when correspond.

Results

Effects of GSNO exposure in *P. extremaustralis*

Nitrosative stress effect on *P. extremaustralis* survival and growth under microaerobic conditions was evaluated using different S-nitrosoglutation (GSNO) concentrations. Growth in the presence of different concentrations of GSNO was similar to the control culture except for 100 μM, which showed a significant decrease ($P<0.05$) at the stationary phase (Fig 1A). Survival assays showed that when the bacterial culture was exposed to GSNO for 1h a significant decrease in bacterial viable counts (CFU/ml) was observed compared with the control culture and provoked a 75% drop in survival in microaerobic cultures (Fig 1B). These results indicate that GSNO exposure affected *P. extremaustralis* survival in a short time. Even though all concentrations tested inhibited survival, only the highest concentration tested affected growth. Therefore, we chose 100 μM GSNO (m-NS) exposure for 1h for further experiments.

Transcriptomic profile of *P. extremaustralis* under low aeration and nitrosative stress conditions

P. extremaustralis response to nitrosative stress was evaluated by comparing transcriptomic data obtained by RNA sequencing (RNAseq) in microaerobic cultures m-C and m-NS. RNA-seq expression profile revealed 5888 transcripts. Rockhopper analysis showed 249 transcripts with differential expression in m-NS compared to m-C ($P<0.05$, $Q<0.05$). Among them, 86 genes were found to be repressed and 163 over-expressed, representing 1.46% and 2.77% of the total, respectively (S2A Fig and S1 Table). Several genes with differential expression did not have defined associated functions and were classified as "hypothetical", representing 11.6% and 21% of the over-expressed and repressed genes, respectively. Among genes with a known predicted function, *P. extremaustralis* under m-NS showed an increased expression of genes involved in carbon, RNA, DNA and iron metabolism (S1 Table).

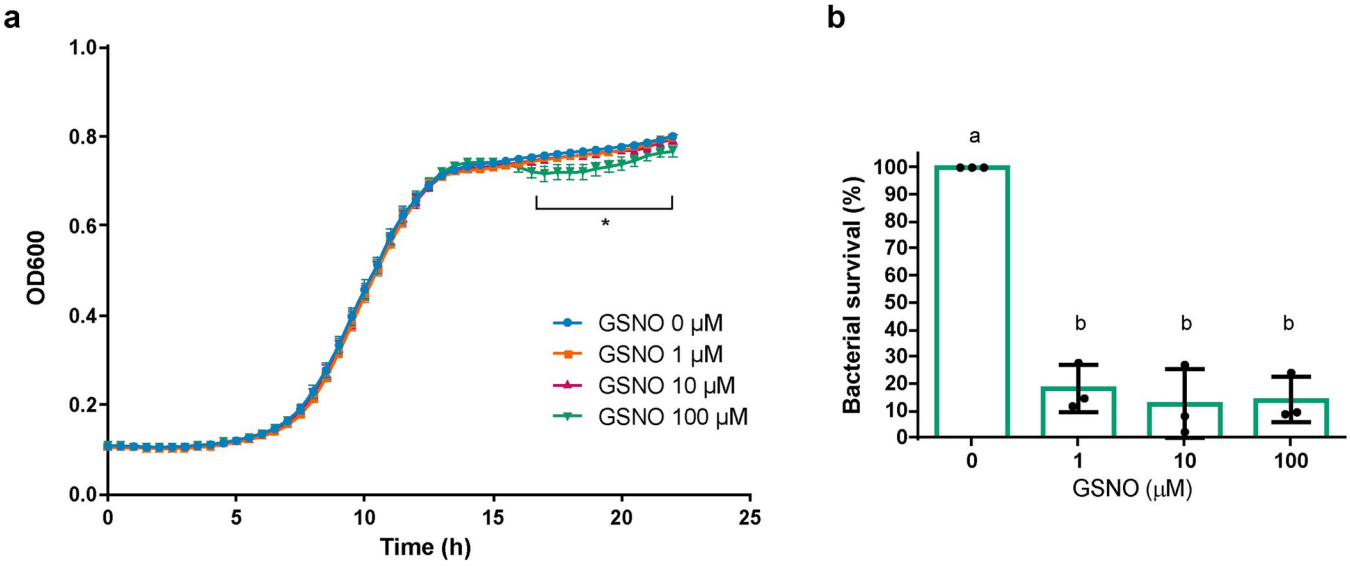

Fig 1. Survival of microaerobic cultures to GSNO exposure. a. Growth curves of *P. extremaustralis* in microaerobiosis with different GSNO concentrations. Values represent the mean ± SD of 6 independent experiments**.** * denotes significant differences using 1-way ANOVA for each time point ($P < 0.05$) **b.** Cultures were exposed to GSNO during 1h and survival in LB plates was determined. Circles represent individual values of independent experiments. Error bars represent the standard deviation of the mean. Different letters denote significant differences using 1-way ANOVA with Tukey's multiple comparisons test ($P < 0.05$).

https://doi.org/10.1371/journal.pone.0301252.g001

RNAseq results were validated by analyzing the expression of three selected genes, *motB*, h*bo* and *flaB* using RT-qPCR (S2B Fig). In concordance with the RNAseq results, we found higher expression levels of *motB*, encoding a flagellar motor rotation protein, in m-NS vs. m-C, whereas we observed a decrease in *hbO*, encoding the hemoglobin-like protein HbO (S2B Fig and S1 Table) and no differences in *flaB* expression between conditions a gene which also did not show expression changes in the global transcriptome analysis.

P. extremaustralis' response to nitrosative stress

To elucidate possible functional relationships, differentially expressed genes were categorized into functional groups (Fig 2A). GSNO exposure caused increased expression of genes encoding different RNS detoxifying enzymes such as an iron-dependent superoxide dismutase (PE143B_0125285) and an alkyl hydroperoxide reductase (*ahpC*), a thioredoxin (PE143B_0111145) and a glutathione S-transferase (PE143B_0109905). A gene encoding another glutathione S-transferase (PE143B_0100180) was repressed in m-NS along with *hbO* (Fig 2A and S1 Table).

Transcriptomic analysis showed an increase in mRNA expression of iron and heme transporters coding genes such as *ctaB*, *ybaN*, *irpA* and *afuA* (Fig 2B and S1 Table). In m-NS we found upregulation in genes related to pyoverdine siderophore biosynthesis, a key function for iron uptake, including *pdvA*, *pdvM*, *pdvF*, *fpvA*, *fpvE* and *fpvK* (Fig 2B and S1 Table).

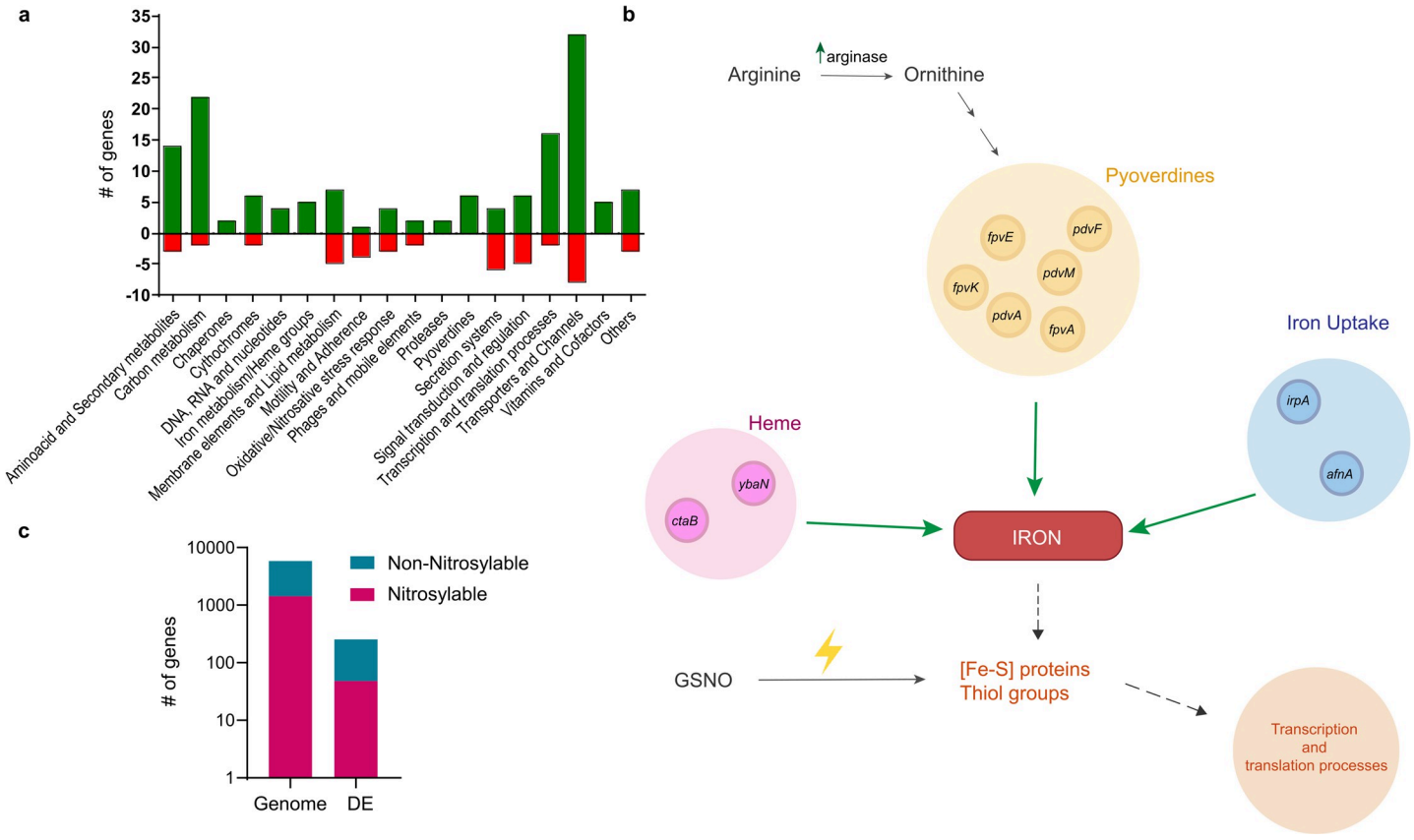

Fig 2. Effect of GSNO on gene expression profile. a. Classification of differentially expressed genes (P<0.05) after GSNO exposure in microaerobiosis (m-NS vs. m-C) into functional categories. Hypothetical transcripts (with no inferred function) are not displayed. Green and red bars represent up- and down-regulated genes, respectively. **b.** Over-expressed genes related to iron metabolism. **c.** Nitrosylable proteins predicted with Target Pathogen in the differential expressed genes compared to total nytrosilable proteins in *P. extremaustralis* genome. DE: Differentially expressed genes. Fisher's exact test, P = 0.0323.

https://doi.org/10.1371/journal.pone.0301252.g002

Moreover, the arginase coding gene, was also upregulated in m-NS comparing with m-C. Arginase catalyzes the conversion of arginine to ornithine, which can then serve as a substrate for pyoverdine biosynthesis (Fig 2B and S1 Table).

Iron and other metals are key components of iron-sulfur proteins that could be target of RNS, leading to protein inactivation and triggering cellular signaling [36]. Therefore, we analyzed other cellular functions related with transcription and protein turn-over. GSNO treated cultures showed an increase in expression of RNA helicase (PE143B_0107010), RNA polymerase associated protein RapA, transcriptional terminator *nusB* (PE143B_0123570) and 11 ribosomal proteins coding genes (S1 Table). In concordance, a gene encoding translation initiation inhibitor was repressed (S1 Table). To deeply analyze the protein turnover related with RNS attack we performed an *in silico* analysis using Target Pathogen platform to detect genes encoding proteins with free tyrosine or cysteine as well as metal binding sites which are reactive to RNS [1]. Among differentially expressed genes in m-NS we found that nitrosylable proteins were over-represented in comparison to non-nitrosylable when total genes of *P. extremaustralis* were considered (Fisher's exact test, P = 0.0323). Overall, our results suggest that nitrosative stress under microaerobic conditions provokes an increase in the expression of genes involved in transcription and translation processes, probably to compensate the damage to proteins with Fe-S clusters or metal binding (Fig 2C).

Inositol metabolism in *P. extremaustralis*

Remarkably, RNAseq results showed increased expression of genes related to inositol catabolism which involves enzymes that convert inositol into acetyl-CoA and dihydroxyacetone phosphate (DHAP) (Fig 3A and S1 Table).

Our results showed a significant up-regulation (P and Q<0.05) in mRNAs encoded in the *iol* operon in response to GSNO stress, including *iolB* (2-fold), *iolD* (1.75-fold), *iolE* (1.83-fold) *iolG2* (also known as *iolW* or *mocA*) (1.86-fold), *iolR* (2.62-fold), and the *iatA* gene (1.75-fold) (Fig 3A and S1 Table). No significant differences were observed in the expression of *iolA* (1-fold), *iolG1*(1.54-fold) nor *iolC/J* (1.25-fold) in both conditions, neither for *iatP* (1.20-fold) and *ibpA* (1.44-fold) (Fig 3A). It was found that *iolC* possesses the DUF2090 domain that was recently proposed to encode 2-deoxy-5-keto-gluconic acid-6-phosphate aldolase [37]. This domain fulfills the function originally attributed to *iolJ*, which is not present in *P. extremaustralis* genome (Fig 3B).

When we compared the inositol catabolic cluster of *P. extremaustralis* with *P. protegens* Pf-5, a well-known plant growth promoter species, and *P. syringae* pv. syringae B728a, a plant pathogen, we found some differences in this genomic region. Unlike *P. protegens* Pf-5, the genome of *P. extremaustralis* did not exhibit the presence of *iolL*. Conversely, we identified a duplication of *iolG* within this bacterial species. *P. syringae* pv. syringae B728a presented *iolH*, which is absent in both *P. protegens* and *P. extremaustralis*. Similar to *P. extremaustralis*, *P. syringae* pv. syringae B728a presented two copies of *iolG* but separated by *iolH* (Fig 3B). The *iolA* gene in *P. extremaustralis* is located in a different genomic region like in *P. protegens* and other analyzed *Pseudomonas* [38]. However, in P. *syringae* pv. syringae B728a, *iolA* is included in the *iol* catabolic cluster (Fig 3B). Furthermore, we found that the *iol* gene cluster of *P. extremaustralis* exhibited a high degree of intraspecific conservation showing the same organization as 14-3b in all genomes analyzed, including strains USBA 515, DSM17835^{T}, 2E-UNGS, CSW01,1906, NQ5.

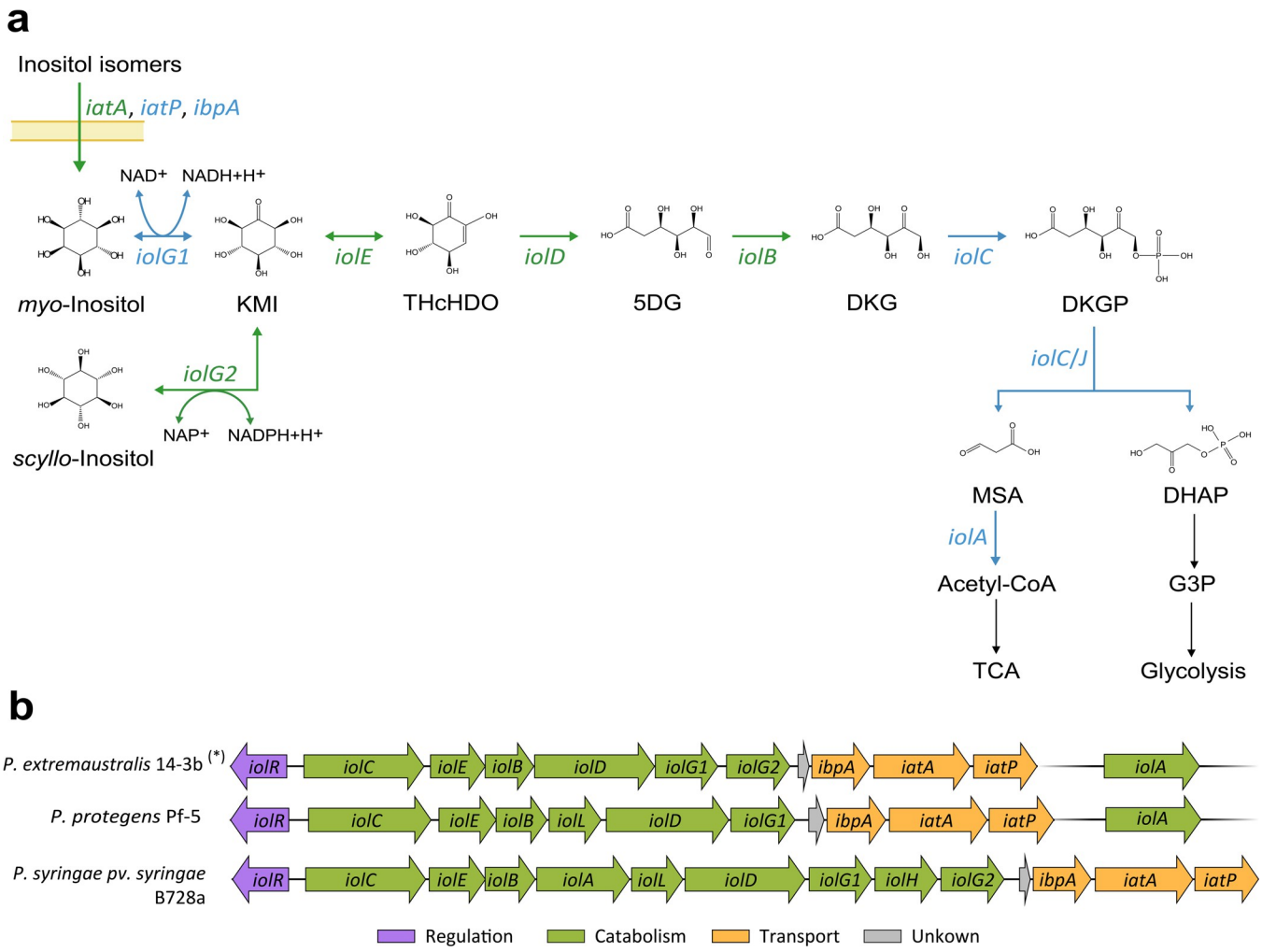

Fig 3. Metabolic pathway associated with inositol catabolism in *Pseudomonas extremaustralis* 14-3b: Expression under nitrosative stress and genetic organization. a. Gene expression and metabolic route related to inositol catabolism under m-NS Genes and arrows shown in green indicate up-regulated functions under m-NS, whereas those in blue represent functions with no expression differences between both conditions. **b**. Analysis of genes involved in inositol in *P. extremaustralis* in comparison with *P. protegens* Pf-5 and *P. syringae* pv. syringae B728a. (*) The same genetic organization was observed in USBA 515, DSM17835^{T}, 2E-UNGS, CSW01,1906 and NQ5 *P. extremaustralis* strains. Compounds: KMI, 2-keto-*myo*-inositol; THcHDO, 3, 3D-(3,4/5) trihydroxycyclohexane-1,2-dione; 5DG, 5-deoxy glucuronic acid; DKG, 2-deoxy-5-keto-d-gluconic acid; DKGP, DKG 6-phosphate; DHAP, dihydroxyacetone phosphate; MSA, malonic semialdehyde; acetyl-CoA, acetyl coenzyme A; DHAP, dihydroxyacetone phosphate; G3P, glyceraldeyde-3-phosphate; TCA, tricarboxylic acid cycle. Genes: *iolG1*, *myo*-inositol dehydrogenase; *iolG2*, *scyllo*-inositol dehydrogenase; *iolE*, 2KMI dehydratase; *iolD*, THcHDO hydrolase; *iolB*, 5DG isomerase; *iolC/J*, DKG kinase + aldolase; *iolA*, MSA dehydrogenase; *iatA*, sugar ABC transporter ATP-binding protein; *iatP*, ABC transporter permease; *ibpA*, sugar ABC transporter substrate-binding protein.

https://doi.org/10.1371/journal.pone.0301252.g003

Use of *myo*-inositol as sole carbon source

Due to the novel finding of the overexpression of inositol catabolism genes in the presence of GSNO and the verification of the complete pathway in *P. extremaustralis* genome, we first tested the capability of this bacterium to grow under aerobic conditions using *myo*-inositol as sole carbon source. Growth was similar between *myo*-inositol and glucose supplemented cultures reaching an OD_{600nm} value of 2.02 ± 0.15 and 2.22 ± 0.15, respectively. Under microaerobic conditions *P. extremaustralis* developed an evident biofilm in *myo*-inositol supplemented cultures (Fig 4A). Therefore, OD_{600nm} and cellular dry weight (DW) were determined (Fig 4B). Similar results were obtained for both carbon sources regardless of the approach employed for growth estimation. Biofilm formation was assayed in E2 medium supplemented

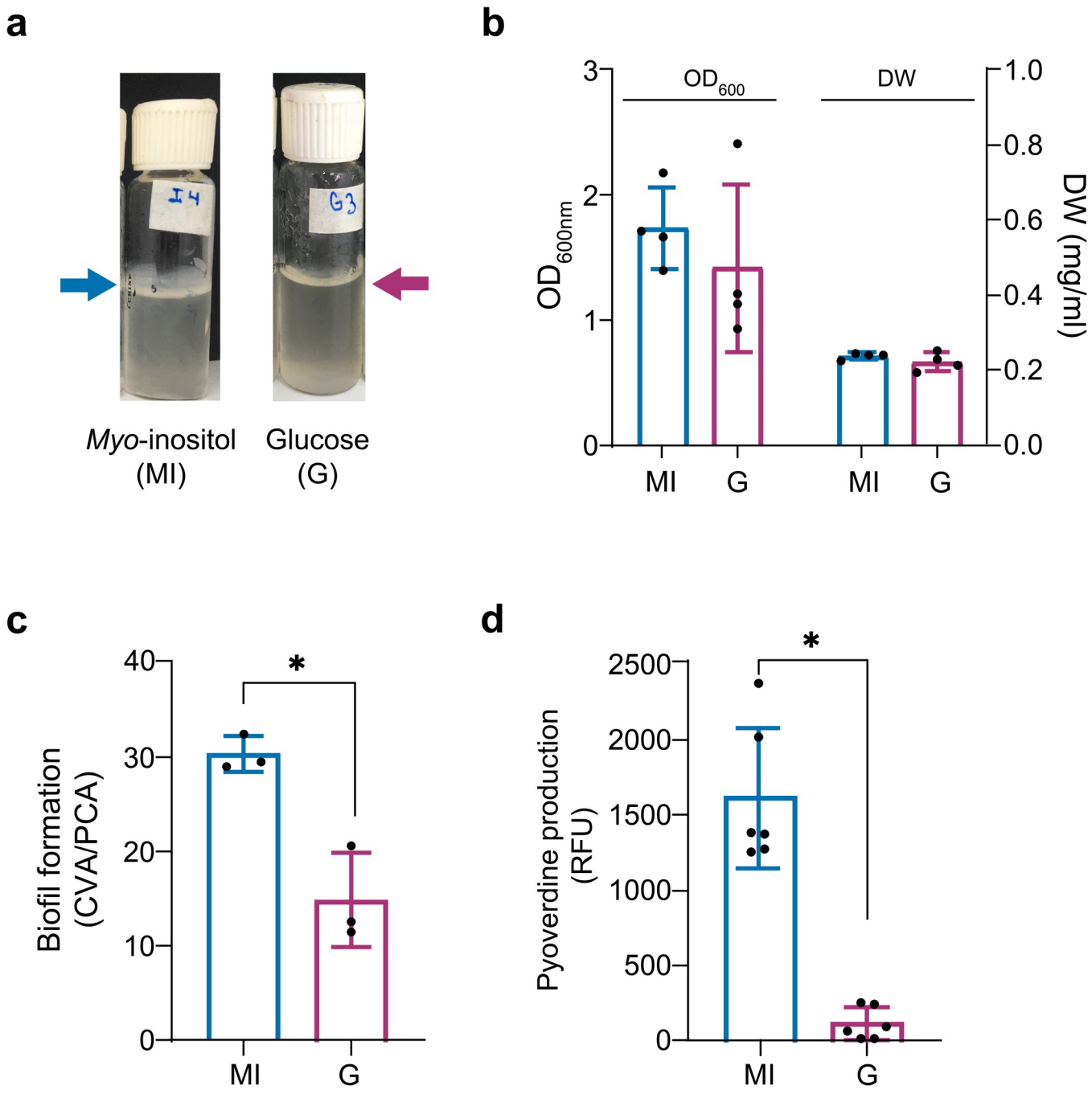

Fig 4. Physiological features of *P. extremaustralis* using *myo*-inositol o glucose as carbon source. a. Photograph of microaerobic *myo*-inositol or glucose supplemented cultures showing the biofilm in the surface. **b.** Microaerobic growth measured by optical density (OD_{600nm}) or Cellular dry weight (DW). **c.** Biofilm formation index (ACV/APC) in *myo*-inositol or glucose. **d.** Effect of carbon sources on pyoverdine production. RFU: Relative Fluorescence Units. Fluorescence units were normalized to the cell dry weight/ml. Error bars represent the standard deviation of the mean. In all cases asterisks (*) indicate significant differences ($P<0.05$) using an Unpaired t- test.

https://doi.org/10.1371/journal.pone.0301252.g004

with glucose or inositol. In concordance, we also found that with *myo*-inositol supplemented cultures *P. extremaustralis* showed a significantly higher biofilm index ($P<0.05$) compared to glucose (Fig 4C).

Additionally, considering the upregulation of coding genes related with pyoverdine biosynthesis after treatment with GSNO, we investigated siderophores production in *P. extremaustralis* using *myo*-inositol as carbon source. Pyoverdine production was significantly higher ($P<0.05$) for *myo*-inositol supplemented cultures comparing to glucose (Fig 4D)

Myo-inositol impact on stress response

Further, we investigated stress resistance when *myo*-inositol was used as sole carbon source under low oxygen conditions. To analyze the nitrosative stress response, we performed a survival test using microaerobic cultures in E2 medium supplemented with *myo*-inositol or glucose exposed to GSNO treatment. We found no differences in survival between those treated with GSNO and control cultures despite of the carbon source (Fig 5A). Additionally, we conducted an assessment of the reduced thiol pool using Mercury Orange in cultures with either inositol or glucose as the carbon source, both with and without GSNO. Our findings indicate

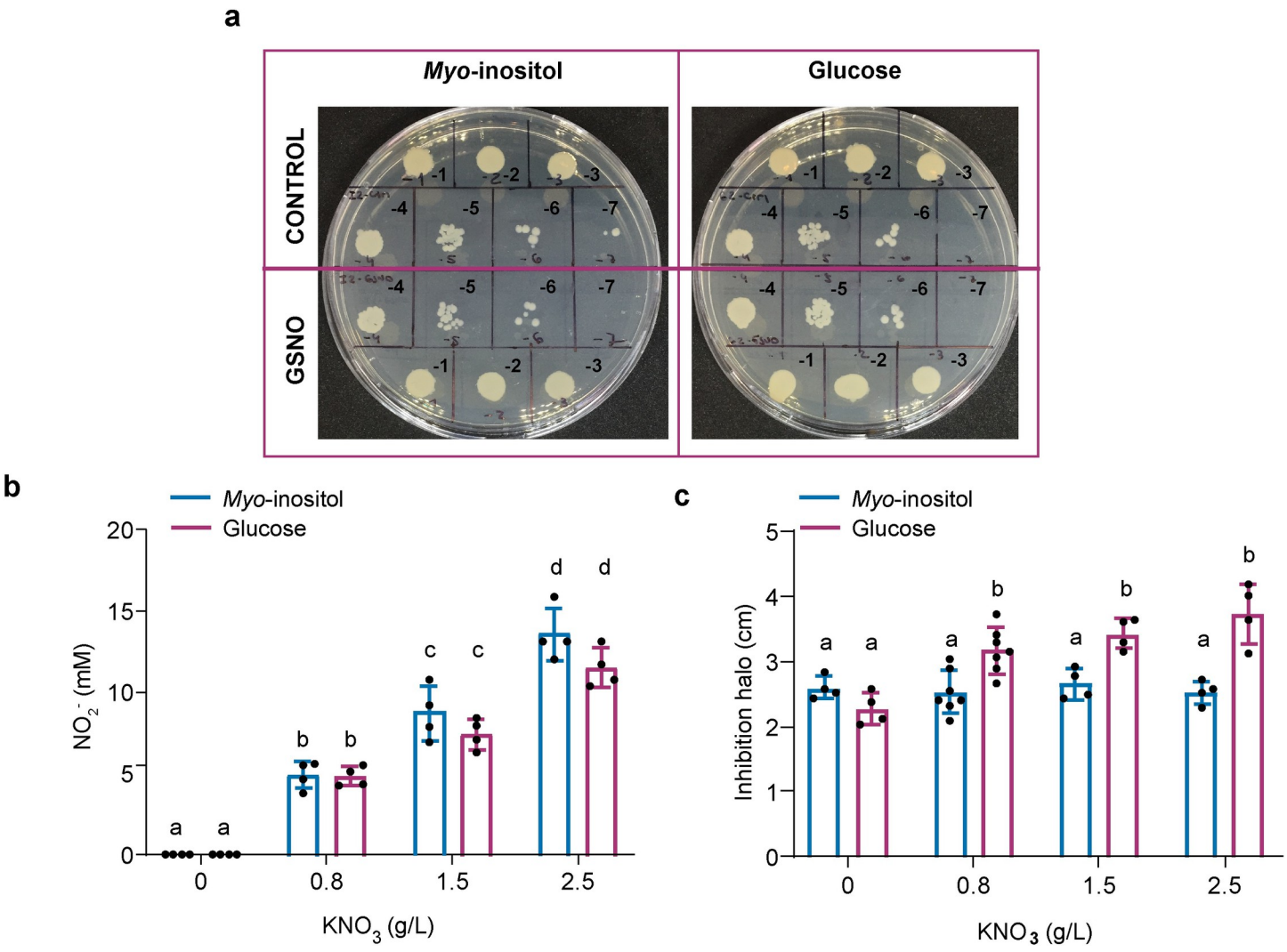

Fig 5. Nitrosative and combined nitro-oxidative stress resistance in *P. extremaustralis*. **a.** Survival after GSNO exposure. **b.** Nitrite production in cultures supplemented with *myo*-inositol or glucose and different nitrate concentrations. **c.** Inhibition halos of cultures performed with *myo*-inositol or glucose at different nitrate concentrations exposed to H_2O_2 (Combined nitro-oxidative stress). Error bars represent the standard deviation of the mean. In all cases, different letters represent significative differences ($P<0.05$) using a 2-Way ANOVA with Tukey's multiple comparisons test.

https://doi.org/10.1371/journal.pone.0301252.g005

that the geometric mean (Gm) for Mercury Orange fluorescence was higher in cultures utilizing inositol compared to those utilizing glucose (S3 Fig). Specifically, the Gm averages were 11740 ± 1419 and 10894 ± 338 for cultures with glucose without and with GSNO, respectively, while the averages for inositol cultures were 10643 ± 2905 and 10268 ± 8380 in stressed cultures with GSNO. This suggests a more reduced state of thiol pool when inositol was employed as the carbon source (S3 Fig). Furthermore, the proportion of positive cells, indicative of those cells exhibiting a positive signal for Mercury Orange, was also higher in inositol cultures, suggesting an increase in the proportion of cells with a cellular state more efficient to handle nitrosative stress when inositol served as the carbon source.

P. extremaustralis is only capable to reduce nitrate to nitrite which accumulates in the extracellular medium. Therefore, the resistance to nitro-oxidative stress derivate from the combination of the nitrite accumulated and H_2O_2 was analyzed in *myo*-inositol and glucose supplemented cultures, following the scheme shown in S4 Fig. Nitrite production was detected in cultures supplemented with *myo*-inositol and glucose as sole carbon source and different nitrate concentrations reaching a maximum of 13.553± 1.624, confirming also the *myo*-inositol utilization in a respiratory pathway (Fig 5B).

When *P. extremaustralis* was grown in *myo*-inositol or glucose supplemented media without nitrate, the oxidative stress resistance was similar for both carbon sources while the nitro-oxidative stress resistance was significantly higher for cultures grown in *myo*-inositol ($P<0.05$) in all tested KNO_3 concentrations (Fig 5C).

Discussion

Bacterial species are subjected to different stress conditions including lack of nutrients, changes in temperature or oxygen availability and oxidative and nitrosative stress, among others. Oxidative and nitrosative stress can be produced by the imbalance between the ROS or RNS generation and the incapability to detoxify them [39].

In response to these stress conditions, bacteria may activate various response mechanisms, such as the production of chaperons and detoxicant enzymes, the adjustment of gene expression, and the modification of their cell envelope composition. A common effect during stress is the reprograming of transcription and translation processes including the reduction of ribosome biogenesis, the modification of the translational machinery and the regulation of initiation and elongation of certain proteins [40]. Interestingly, gene expression during stress involves not only the transcription processes but also the modification of mRNA stability and in overall with translation provokes a transcriptome stability [41,42]. In this work, we found an up-regulation of the transcription and translation machinery probably to compensate the damage caused by RNS particularly on nitrosylable proteins. The Fe-S clusters, that can be found in three different forms, exhibit high capacity of accepting or donating electrons thus are important for redox response and act as redox sensors like the Fnr regulator in *Escherichia coli* or Anr in *Pseudomonas* species [43–45].These proteins and others containing metals are involved in several essential cellular functions, like respiration, central carbon catabolism and RNA and DNA processes, and they are targets of dagame induced by RNS [43] Particularly, it has been reported that the reaction between nitric oxide (NO) with Fe-S clusters lead to protein degradation and breakdown of the cluster generating dinitrosyl iron complexes [46]. Our analysis using Target Pathogen platform predicted the enrichment of genes encoding nitrosylable proteins in the differentially expressed ones, particularly in those upregulated. Even though these findings require more experimental evidences, our hypothesis is that to cope with GSNO derived stress the Fe-S and metal binding proteins need to be replaced. This also could explain the upregulation of Fe-uptake related genes observed in presence of GSNO. Iron

is involved in the Fenton reaction in presence of H_2O_2, derived from endogenous or exogenous sources, which could exacerbate the oxidative damage but paradoxically this metal is also necessary for Fe-S and metal protein biogenesis [47,48]. This complex scenario additionally requires the involvement of enzymes and antioxidant cycles. In presence of GSNO we found upregulated the coding genes of glutathione S-transferase, superoxide dismutase (SOD), thiol-disulfide isomerase, thioredoxins and alkyl hydroperoxide reductase subunit C-like protein. The alkyl hydroperoxide reductase, important during non-lethal stress, SOD as well as the oxidation of thioredoxins in response to oxidative stress depends on NAD(P)H availability and in overall reduction power is needed for the essential process for survival and to cope with stress [49]. Interestingly, the needed of NADH and/or NADPH production during stress could represent a challenge for bacterial cells. Glycolysis and TCA provides the NADH and energy necessaries for bacterial survival but also creates an oxidative scenario through the respiration chain [50]. It has been reported several metabolic strategies to obtain energy and reducing power besides glycolysis such as amino acid catabolism, ethanol oxidation and in *P. fluorescens* an entire metabolic reprogramming has been reported in presence of oxidative stress to generate NADPH [51]. In this previous work the authors showed an increase in the activity and expression of malic enzyme (similar to this work in presence of GSNO), glucose-6-phosphate dehydrogenase and NADP+-isocitrate dehydrogenase [51].

In addition, we found that in presence of GSNO under microaerobic conditions *P. extremaustralis* over-expressed several *iol* catabolic genes including the transcriptional regulator and the *iatA* gene. We also demonstrated that this bacterium was effectively capable of using inositol as its sole carbon source. Inositol is a sugar alcohol present in all domains of life and presents various structural isomers [52], with *myo*-inositol being the most abundant in nature. *Myo*-inositol is found in high quantities in plants, including root exudates, and may also originate from the dephosphorylation of phytate, one of the major phosphorus storage molecules for plants [53]. Inositol catabolism has been experimentally demonstrated in several bacterial species, both Gram positive and Gram negative, belonging to genera such as *Rhizobium*, *Lactobacillus*, *Klebsiella*, *Corynebacterium*, *Legionella*, *Bacillus*, *and Salmonella* [54–60]. Furthermore, an extensive analysis of inositol catabolic genes in thousands of bacterial genomes revealed a widespread distribution within different ecological niches [53]. While inositol metabolism in bacteria has garnered recent attention, its role in stress resistance remains unexplored. Remarkably, our findings revealed that inositol protects against nitro-oxidative stress, and increases biofilm and pyoverdine production, which are relevant traits for environmental adaptability. Inositol catabolism leads to the production of glyceraldehyde-3 phosphate, and acetyl-CoA both intermediaries of central energy generation metabolism. In addition, *iolG2*, which was found overexpressed after GSNO exposure, is related to NADPH generation, necessary for the function of antioxidative defenses. Additionally, a trend to display a higher thiol pool was shown in cells growing in inositol as carbon source was observed compared with glucose. Low-molecular-weight thiols are a heterogeneous group of molecules with a highly reactive sulfhydryl group present in the different groups of living cells [61]. The most representative members of this group include glutathione, cysteine and coenzyme A [62]. These compounds participate in several redox related functions such as homeostasis, maintenance of proteins structure and the detoxification of ROS or RNS through the action of thiol-dependent enzymes such as disulfide reductases, peroxiredoxins, glutaredoxins, and thiol transferases [62]. Thus, although no significant in the analyzed conditions, the increment of the reduced state of thiol pool that inositol catabolism in nature could resulted an advantage in the environment under this stress conditions.

It is worth noting that previous transcriptome analysis of *P. extremaustralis* performed under cold conditions or under microaerobic conditions with or without oxidative stress did

not show the upregulation of inositol catabolic genes [14,63,64], indicating a fine-tuning response to nitrosative stress.

Principio del formulario

Some RNS also play a crucial role in cell signaling. For instance, in plants, NO mediates for various processes including root hair growth, stomatal closure, programmed cell death and other responses that help them adapt to changing environmental conditions [8] whereas in bacteria, NO plays a role as intermediary in denitrification processes, but also in biofilm formation and quorum sensing [65]. The *iol* gene cluster was identified in both plant-pathogenic bacteria, and rhizospheric plant growth promoting bacteria forming symbiotic root nodules [53].

Recently, the *iol* gene cluster in *Pseudomonas* was identified as an important trait in root colonizers, by increasing swimming motility and siderophore production in response to plant derived inositol [38]. Increased pyoverdine siderophore production in presence of *myo*-inositol was also observed in this work. *P. extremaustralis* possesses plant growth-promotion traits, including the ability to solubilize phosphate and produce indole acetic acid [66]. Since NO is also a signaling molecule released by plants [67], we hypothesize that NO released by GSNO mimic the NO production of plants, triggering the differential expression of the inositol metabolic pathway conferring an adaptive advantage.

In conclusion, our findings reveal a multifaceted and finely tuned response mechanism to nitrosative stress that encompasses transcriptional reprogramming, the upregulation of genes encoding key proteins involved in iron homeostasis, and the activation of inositol catabolism. Notably, experimental results point to inositol metabolism as a novel mechanism to cope with stress.

Supporting information

S1 Fig. Transcriptome data information. Quality summary of sequencing data (a) and dot plot representing normalized counts for each RNAseq replicate in microaerobic culture conditions (b) and microaerobic culture subjected to GSNO (m-NS) (c).
(PDF)

S2 Fig. GSNO effect on gene expression. a. Volcano plots depicting–$\log_{10}$ (Q-value) versus $\log_2$ (Fold Change -FC-). Differentially expressed genes (DEGs) are represented by colored dots. Green dots represent upregulated genes (P-value and Q-value <0.05, Fold change >1.5) and red dots represent downregulated genes (P-value and Q-value <0.05, Fold change < -1.5) in presence of GSNO. For the construction of the Volcano plots, genes were initially filtered based on their P-values. All resulting genes were plotted and filtered again by Q-value. b. Quantitative Real Time PCR. Comparative expression analysis of 3 selected genes between m-NS and microaerobic growth conditions. Values represent the mean ± SD of three independent experiments.
(PDF)

S3 Fig. GSNO effect on the reduced thiol pool. Flow cytometry assays using Mercury Orange in cultures with glucose (G) or myo-inositol (MI) as the sole carbon source, with or without GSNO. a. Geometric mean (Gm) for Mercury Orange fluorescence b. Proportion of cells which present positive signal for Mercury Orange, calculated using a non-stained control.
(PDF)

S4 Fig. Nitro-oxidative stress assay. Scheme of the experimental design used to study the resistance to nitro-oxidative stress derivate from the combination of the nitrite accumulated

and H_2O_2.
(PDF)

S1 Table. Effect of GSNO on gene expression of *Pseudomonas extremaustralis*. Differentially expressed genes by functional category and fold change. Genes predicted as nitrosilation blank are indicated (X). Genes involved in inositol metabolism are indicated in bold.
(XLSX)

Acknowledgments

We are thankful to Dr. Jörg Vogel (Institut für Molekulare Infektionsbiologie (IMIB)–University of Würzburg) for his guidance and for providing resources for conducting the RNAseq experiments. E.C.S.V. received a Deutscher Akademischer Austauschdienst (DAAD) fellowship for short-term research stays at the RNA biology group (IMIB–University of Würzburg, Germany). DFdP, NIL and PMT are career investigators from Consejo Nacional de Investigaciones Cientificas y Tecnicas (CONICET, Argentina).

Author Contributions

Conceptualization: Esmeralda C. Solar Venero, Nancy I. López, Paula M. Tribelli.

Data curation: Ezequiel Sosa.

Formal analysis: Esmeralda C. Solar Venero, Lucia Giambartolomei, Ezequiel Sosa, Darío Fernández do Porto, Nancy I. López, Paula M. Tribelli.

Funding acquisition: Nancy I. López, Paula M. Tribelli.

Investigation: Esmeralda C. Solar Venero, Lucia Giambartolomei.

Project administration: Paula M. Tribelli.

Resources: Paula M. Tribelli.

Supervision: Darío Fernández do Porto, Paula M. Tribelli.

Visualization: Esmeralda C. Solar Venero, Paula M. Tribelli.

Writing – original draft: Esmeralda C. Solar Venero, Lucia Giambartolomei, Nancy I. López, Paula M. Tribelli.

References

1. Crack JC, Thomson AJ, Brun NE Le. Iron − Sulfur Clusters as Biological Sensors: The Chemistry of Reactions with Molecular Oxygen and Nitric Oxide. 2014.
2. Czaja AJ. Immunopathogenesis of Autoimmune Liver Damage. 2017. pp. 19–48. https://doi.org/10.1016/B978-0-444-63707-9.00002–7
3. Tharmalingam S, Alhasawi A, Appanna VP, Lemire J, Appanna VD. Reactive nitrogen species (RNS)-resistant microbes: adaptation and medical implications. Biol Chem. 2017; 398: 1193–1208. https://doi.org/10.1515/hsz-2017-0152 PMID: 28622140
4. Aranda-Rivera AK, Cruz-Gregorio A, Arancibia-Hernández YL, Hernández-Cruz EY, Pedraza-Chaverri J. RONS and Oxidative Stress: An Overview of Basic Concepts. Oxygen. 2022; 2: 437–478. https://doi.org/10.3390/oxygen2040030
5. Lelieveld S, Wilson J, Dovrou E, Mishra A, Lakey PSJ, Shiraiwa M, et al. Hydroxyl Radical Production by Air Pollutants in Epithelial Lining Fluid Governed by Interconversion and Scavenging of Reactive Oxygen Species. Cite This: Environ Sci Technol. 2021; 55: 14069–14079. https://doi.org/10.1021/acs.est.1c03875 PMID: 34609853
6. Li H, Zhou X, Huang Y, Liao B, Cheng L, Ren B. Reactive Oxygen Species in Pathogen Clearance: The Killing Mechanisms, the Adaption Response, and the Side Effects. Front Microbiol. 2020; 11: 622534. https://doi.org/10.3389/fmicb.2020.622534 PMID: 33613470

7. Del Río LA. ROS and RNS in plant physiology: an overview. 2015. J Exp Bot. 2015; 66:2827–37. https://doi.org/10.1093/jxb/erv099 PMID: 25873662

8. Zaffagnini M, Bedhomme M, Marchand CH, Morisse S, Trost P, Lemaire SD. Redox Regulation in Photosynthetic Organisms: Focus on Glutathionylation. https://home.liebertpub.com/ars. 2012; 16: 567–586. https://doi.org/10.1089/ARS.2011.4255 PMID: 22053845

9. Robinson JL, Adolfsen KJ, Brynildsen MP. Deciphering nitric oxide stress in bacteria with quantitative modeling. Curr Opin Microbiol. 2014; 19: 16–24. https://doi.org/10.1016/j.mib.2014.05.018 PMID: 24983704

10. Arai H. Regulation and Function of Versatile Aerobic and Anaerobic Respiratory Metabolism in *Pseudomonas aeruginosa*. Front Microbiol. 2011; 2: 103. https://doi.org/10.3389/fmicb.2011.00103 PMID: 21833336

11. Tribelli PM, Lujan AM, Pardo A, Ibarra JG, Fernández Do Porto D, Smania A, et al. Core regulon of the global anaerobic regulator Anr targets central metabolism functions in Pseudomonas species. Sci Rep. 2019; 9: 9065. https://doi.org/10.1038/s41598-019-45541-0 PMID: 31227753

12. Raiger Iustman LJ, Tribelli PM, Ibarra JG, Catone M V, Solar Venero EC, López NI. Genome sequence analysis of *Pseudomonas extremaustralis* provides new insights into environmental adaptability and extreme conditions resistance. Extremophiles. 2015; 19: 207–220. https://doi.org/10.1007/s00792-014-0700-7 PMID: 25316211

13. Fonseca P, Moreno R, Rojo F. Growth of *Pseudomonas putida* at low temperature: Global transcriptomic and proteomic analyses. Environ Microbiol Rep. 2011. https://doi.org/10.1111/j.1758-2229.2010.00229.x PMID: 23761279

14. Tribelli PM, Solar Venero EC, Ricardi MM, Gómez-Lozano M, Raiger Iustman LJ, Molin S, et al. Novel Essential Role of Ethanol Oxidation Genes at Low Temperature Revealed by Transcriptome Analysis in the Antarctic Bacterium Pseudomonas extremaustralis. PLoS One. 2015; 10: e0145353. https://doi.org/10.1371/journal.pone.0145353 PMID: 26671564

15. da Cruz Nizer WS, Inkovskiy V, Versey Z, Strempel N, Cassol E, Overhage J. Oxidative Stress Response in Pseudomonas aeruginosa. Pathogens. 2021; 10: 1187. https://doi.org/10.3390/pathogens10091187 PMID: 34578219

16. López NI, Pettinari MJ, Stackebrandt E, Tribelli PM, Põtter M, Steinbüchel A, et al. Pseudomonas extremaustralis sp. nov., a Poly(3-hydroxybutyrate) producer isolated from an antarctic environment. Curr Microbiol. 2009; 59: 514–519. https://doi.org/10.1007/s00284-009-9469-9 PMID: 19688380

17. Rio DC, Ares M, Hannon GJ, Nilsen TW. Purification of RNA using TRIzol (TRI Reagent). Cold Spring Harb Protoc. 2010;5. https://doi.org/10.1101/pdb.prot5439 PMID: 20516177

18. Bolger AM, Lohse M, Usadel B. Trimmomatic: a flexible trimmer for Illumina sequence data. Bioinformatics. 2014; 30: 2114–2120. https://doi.org/10.1093/bioinformatics/btu170 PMID: 24695404

19. Tjaden B. A computational system for identifying operons based on RNA-seq data. Methods. 2020; 176: 62–70. https://doi.org/10.1016/j.ymeth.2019.03.026 PMID: 30953757

20. Ogata H, Goto S, Sato K, Fujibuchi W, Bono H, Kanehisa M. KEGG: Kyoto Encyclopedia of Genes and Genomes. Nucleic Acids Res. 1999; 27: 29–34. https://doi.org/10.1093/nar/27.1.29 PMID: 9847135

21. Caspi R, Billington R, Ferrer L, Foerster H, Fulcher CA, Keseler IM, et al. The MetaCyc database of metabolic pathways and enzymes and the BioCyc collection of pathway/genome databases. Nucleic Acids Res. 2016; 44: D471–480. https://doi.org/10.1093/nar/gkv1164 PMID: 26527732

22. Szklarczyk D, Gable AL, Lyon D, Junge A, Wyder S, Huerta-Cepas J, et al. STRING v11: protein–protein association networks with increased coverage, supporting functional discovery in genome-wide experimental datasets. Nucleic Acids Res. 2019; 47: D607–D613. https://doi.org/10.1093/nar/gky1131 PMID: 30476243

23. Sosa EJ, Burguener G, Lanzarotti E, Defelipe L, Radusky L, Pardo AM, et al. Target-Pathogen: a structural bioinformatic approach to prioritize drug targets in pathogens. Nucleic Acids Res. 2018; 46: D413–D418. https://doi.org/10.1093/nar/gkx1015 PMID: 29106651

24. Altschul S. Gapped BLAST and PSI-BLAST: a new generation of protein database search programs. Nucleic Acids Res. 1997; 25: 3389–3402. https://doi.org/10.1093/nar/25.17.3389 PMID: 9254694

25. Aziz RK, Bartels D, Best AA, DeJongh M, Disz T, Edwards RA, et al. The RAST Server: Rapid Annotations using Subsystems Technology. BMC Genomics. 2008; 9: 75. https://doi.org/10.1186/1471-2164-9-75 PMID: 18261238

26. Winsor GL, Griffiths EJ, Lo R, Dhillon BK, Shay JA, Brinkman FSL. Enhanced annotations and features for comparing thousands of Pseudomonas genomes in the *Pseudomonas* genome database. Nucleic Acids Res. 2016; 44: D646–53. https://doi.org/10.1093/nar/gkv1227 PMID: 26578582

27. Livak KJ, Schmittgen TD. Analysis of Relative Gene Expression Data Using Real-Time Quantitative PCR and the 2−ΔΔCT Method. Methods. 2001; 25: 402–408. https://doi.org/10.1006/meth.2001.1262 PMID: 11846609

28. Lageveen RG, Huisman GW, Preusting H, Ketelaar P, Eggink G, Witholt B. Formation of Polyesters by Pseudomonas oleovorans: Effect of Substrates on Formation and Composition of Poly- (R)-3-Hydroxyalkanoates and Poly- (R)-3-Hydroxyalkenoates. Appl Environ Microbiol. 1988; 54: 2924–2932. https://doi.org/10.1128/aem.54.12.2924-2932.1988 PMID: 16347790

29. O'Toole GA, Kolter R. Flagellar and twitching motility are necessary for *Pseudomonas aeruginosa* biofilm development. Mol Microbiol. 1998; 30: 295–304. https://doi.org/10.1046/j.1365-2958.1998.01062.x PMID: 9791175

30. Ruiz JA, Bernar EM, Jung K. Production of Siderophores Increases Resistance to Fusaric Acid in Pseudomonas protegens Pf-5. Devireddy lax, editor. PLoS One. 2015; 10: e0117040. https://doi.org/10.1371/journal.pone.0117040 PMID: 25569682

31. Olmo A Del, Caramelo C, Sanjose C. Fluorescent complex of pyoverdin with aluminum. J Inorg Biochem. 2003; 97: 384–387. https://doi.org/10.1016/s0162-0134(03)00316-7 PMID: 14568244

32. Ayub ND, Pettinari MJ, Ruiz JA, López NI. A polyhydroxybutyrate-producing *Pseudomonas sp*. isolated from antarctic environments with high stress resistance. Curr Microbiol. 2004; 49: 170–174. https://doi.org/10.1007/s00284-004-4254-2 PMID: 15386099

33. Schneider CA, Rasband WS, Eliceiri KW. NIH Image to ImageJ: 25 years of image analysis. Nat Methods. 2012; 9: 671–675. Available: http://www.ncbi.nlm.nih.gov/pubmed/22930834. https://doi.org/10.1038/nmeth.2089 PMID: 22930834

34. Gerhard P, Murray R, Costilow N, Nester W, Wood N, Krieg N, et al. Manual of Method of General Bacteriology. Washington: American Society for microbiology; 1981.

35. Thomas M, Nicklee T, Hedley DW. Differential effects of depleting agents on cytoplasmic and nuclear non-protein sulphydryls: a fluorescence image cytometry study. Br J Cancer. 1995; 72: 45. https://doi.org/10.1038/bjc.1995.275 PMID: 7599065

36. Seth D, Hausladen A, Stamler JS. Anaerobic Transcription by OxyR: A Novel Paradigm for Nitrosative Stress. Antioxid Redox Signal. 2020; 32: 803–816. https://doi.org/10.1089/ars.2019.7921 PMID: 31691575

37. Price MN, Deutschbauer AM, Arkin AP. Filling gaps in bacterial catabolic pathways with computation and high-throughput genetics. PLoS Genet. 2022; 18: e1010156. https://doi.org/10.1371/journal.pgen.1010156 PMID: 35417463

38. Sánchez-Gil JJ, Poppeliers SWM, Vacheron J, Zhang H, Odijk B, Keel C, et al. The conserved iol gene cluster in *Pseudomonas* is involved in rhizosphere competence. Current Biology. 2023; 33: 3097–3110. e6. https://doi.org/10.1016/j.cub.2023.05.057 PMID: 37419116

39. Chautrand T, Souak D, Chevalier S, Duclairoir-Poc C. Gram-Negative Bacterial Envelope Homeostasis under Oxidative and Nitrosative Stress. Microorganisms. 2022;10. https://doi.org/10.3390/microorganisms10050924 PMID: 35630368

40. Advani VM, Ivanov P. Translational Control under Stress: Reshaping the Translatome. BioEssays. 2019;41. https://doi.org/10.1002/bies.201900009 PMID: 31026340

41. Kristoffersen SM, Haase C, Weil MR, Passalacqua KD, Niazi F, Hutchison SK, et al. Global mRNA decay analysis at single nucleotide resolution reveals segmental and positional degradation patterns in a Gram-positive bacterium. Genome Biol. 2012; 13: R30. https://doi.org/10.1186/gb-2012-13-4-r30 PMID: 22537947

42. Vargas-Blanco DA, Shell SS. Regulation of mRNA Stability During Bacterial Stress Responses. Front Microbiol. 2020; 11: 2111. https://doi.org/10.3389/fmicb.2020.02111 PMID: 33013770

43. Vernis L, El Banna N, Baïlle D, Hatem E, Heneman A, Huang M-E. Fe-S Clusters Emerging as Targets of Therapeutic Drugs. Oxid Med Cell Longev. 2017; 2017: 3647657. https://doi.org/10.1155/2017/3647657 PMID: 29445445

44. Golinelli-Cohen M-P, Bouton C. Fe-S Proteins Acting as Redox Switch: New Key Actors of Cellular Adaptive Responses. Curr Chem Biol. 2017;11. https://doi.org/10.2174/2212796811666170406163809

45. Galimand M, Gamper M, Zimmermann A, Haas D. Positive FNR-like control of anaerobic arginine degradation and nitrate respiration in *Pseudomonas aeruginosa*. J Bacteriol. 1991; 173: 1598–606. Available: http://www.ncbi.nlm.nih.gov/pubmed/1900277.

46. Harrop TC, Tonzetich ZJ, Reisner E, Lippard SJ. Reactions of synthetic [2Fe-2S] and [4Fe-4S] clusters with nitric oxide and nitrosothiols. J Am Chem Soc. 2008; 130: 15602–10. https://doi.org/10.1021/ja8054996 PMID: 18939795

47. Reniere ML. Reduce, Induce, Thrive: Bacterial Redox Sensing during Pathogenesis. J Bacteriol. 2018;200. https://doi.org/10.1128/JB.00128-18 PMID: 29891640

48. Winterbourn CC. Toxicity of iron and hydrogen peroxide: the Fenton reaction. Toxicol Lett. 1995;82–83: 969–74. https://doi.org/10.1016/0378-4274(95)03532-x PMID: 8597169

49. Lemire J, Alhasawi A, Appanna VP, Tharmalingam S, Appanna VD. Metabolic defence against oxidative stress: the road less travelled so far. J Appl Microbiol. 2017; 123: 798–809. https://doi.org/10.1111/jam.13509 PMID: 28609580

50. Zhang J, Li X, Olmedo M, Holdorf AD, Shang Y, Artal-Sanz M, et al. A Delicate Balance between Bacterial Iron and Reactive Oxygen Species Supports Optimal C. elegans Development. Cell Host Microbe. 2019; 26: 400–411.e3. https://doi.org/10.1016/j.chom.2019.07.010 PMID: 31444089

51. Singh R, Mailloux RJ, Puiseux-Dao S, Appanna VD. Oxidative stress evokes a metabolic adaptation that favors increased NADPH synthesis and decreased NADH production in *Pseudomonas fluorescens*. J Bacteriol. 2007; 189: 6665–75. https://doi.org/10.1128/JB.00555-07 PMID: 17573472

52. Michell RH. Inositol derivatives: evolution and functions. Nat Rev Mol Cell Biol. 2008; 9: 151–161. https://doi.org/10.1038/nrm2334 PMID: 18216771

53. Weber M, Fuchs TM. Metabolism in the Niche: a Large-Scale Genome-Based Survey Reveals Inositol Utilization To Be Widespread among Soil, Commensal, and Pathogenic Bacteria. Microbiol Spectr. 2022; 10: e0201322. https://doi.org/10.1128/spectrum.02013-22 PMID: 35924911

54. Fry J, Wood M, Poole PS. Investigation of *myo* -Inositol Catabolism in *Rhizobium leguminosarum* bv. *viciae* and Its Effect on Nodulation Competitiveness. Molecular Plant-Microbe Interactions®. 2001; 14: 1016–1025. https://doi.org/10.1094/MPMI.2001.14.8.1016 PMID: 11497462

55. Yebra MJ, Zúñiga M, Beaufils S, Pérez-Martínez G, Deutscher J, Monedero V. Identification of a Gene Cluster Enabling *Lactobacillus casei* BL23 To Utilize *myo* -Inositol. Appl Environ Microbiol. 2007; 73: 3850–3858. https://doi.org/10.1128/AEM.00243-07 PMID: 17449687

56. Krings E, Krumbach K, Bathe B, Kelle R, Wendisch VF, Sahm H, et al. Characterization of *myo* -Inositol Utilization by *Corynebacterium glutamicum*: the Stimulon, Identification of Transporters, and Influence on l -Lysine Formation. J Bacteriol. 2006; 188: 8054–8061. https://doi.org/10.1128/JB.00935-06 PMID: 16997948

57. Morinaga T, Ashida H, Yoshida K-I. Identification of two scyllo-inositol dehydrogenases in *Bacillus subtilis*. Microbiology (Reading). 2010; 156: 1538–1546. https://doi.org/10.1099/mic.0.037499–0

58. Yuan C, Yang P, Wang J, Jiang L. Myo-inositol utilization by *Citrobacter koseri* promotes brain infection. Biochem Biophys Res Commun. 2019; 517: 427–432. https://doi.org/10.1016/j.bbrc.2019.07.112 PMID: 31376937

59. Manske C, Schell U, Hilbi H. Metabolism of *myo* -Inositol by *Legionella pneumophila* Promotes Infection of Amoebae and Macrophages. Appl Environ Microbiol. 2016; 82: 5000–5014. https://doi.org/10.1128/AEM.01018-16 PMID: 27287324

60. Kröger C, Rothhardt JE, Brokatzky D, Felsl A, Kary SC, Heermann R, et al. The small RNA RssR regulates myo-inositol degradation by *Salmonella enterica*. Sci Rep. 2018; 8: 17739. https://doi.org/10.1038/s41598-018-35784-8 PMID: 30531898

61. Tossounian M-A, Zhao Y, Yu BYK, Markey SA, Malanchuk O, Zhu Y, et al. Low-molecular-weight thiol transferases in redox regulation and antioxidant defence. Redox Biol. 2024; 103094. https://doi.org/10.1016/j.redox.2024.103094 PMID: 38479221

62. Van Laer K, Hamilton CJ, Messens J. Low-Molecular-Weight Thiols in Thiol–Disulfide Exchange. https://home.liebertpub.com/ars. 2013; 18: 1642–1653. https://doi.org/10.1089/ARS.2012.4964 PMID: 23075082

63. Tribelli PM, Rossi L, Ricardi MM, Gomez-Lozano M, Molin S, Raiger Iustman LJ, et al. Microaerophilic alkane degradation in *Pseudomonas extremaustralis*: a transcriptomic and physiological approach. J Ind Microbiol Biotechnol. 2018; 45: 15–23. https://doi.org/10.1007/s10295-017-1987-z PMID: 29116430

64. Solar Venero EC, Ricardi MM, Gomez-Lozano M, Molin S, Tribelli PM, López NI. Oxidative stress under low oxygen conditions triggers hyperflagellation and motility in the Antarctic bacterium *Pseudomonas extremaustralis*. Extremophiles. 2019;23. https://doi.org/10.1007/s00792-019-01110-x PMID: 31250111

65. Williams DE, Boon EM. Towards Understanding the Molecular Basis of Nitric Oxide-Regulated Group Behaviors in Pathogenic Bacteria. J Innate Immun. 2019; 11: 205–215. https://doi.org/10.1159/000494740 PMID: 30557874

66. Ibarra JG. Estudios microbiológicos relacionados con el mejoramiento de cultivos vegetales en zonas desfavorables. Doctoral Thesis, Facultad de Ciencias Exactas y Natural. 2017.

67. Sasaki Y, Oguchi H, Kobayashi T, Kusama S, Sugiura R, Moriya K, et al. Nitrogen oxide cycle regulates nitric oxide levels and bacterial cell signaling. Sci Rep. 2016; 6: 22038. https://doi.org/10.1038/srep22038 PMID: 26912114